 doi:10.20944/preprints202209.0162.v1

Review

Bi-substituted Ferrite Garnet Type Magneto-Optic Materials Studied at ESRI Nano-Fabrication Laboratories, ECU, Australia

Mohammad Nur-E-Alam [1*], Mikhail Vasiliev [2] and Kamal Alameh [3]

[1] School of Science, Edith Cowan University, 270 Joondalup Drive, Joondalup, WA 6027, Australia; m.nur-e-alam@ecu.edu.au
[2] ClearVue Technologies Limited, Unit 7/567 Newcastle St, West Perth WA 6005, Australia; vasiliev.mikhail@gmail.com
[3] Alpha Solar Tech., WA 6105, Australia; kalameh@bigpond.net.au
* Correspondence: m.nur-e-alam@ecu.edu.au

Abstract: Since 2007, at the Electron Science Research Institute (ESRI) nano-fabrication laboratories, Edith Cowan University, Australia, we have devoted research efforts to the synthesis and characterization of bismuth-containing ferrite-garnet-type thin-film magneto-optic (MO) materials of different compositions. We report on the development and properties of highly bismuth-substituted iron-garnet thin films prepared by using radio frequency (RF) magnetron sputtering. We study the process parameters associated with the RF magnetron sputter deposition technique and investigate the results of optimizing process parameters and implementing several special techniques including the fabrication of co-sputtered nanocomposite films, all-garnet multilayer structures, applying oxygen plasma treatment on amorphous garnet layers just after the deposition process, and designing modifications of the annealing crystallization process and regimes for achieving the best MO properties. We demonstrated significant improvement in MO properties of Bi-containing ferrite-type garnet thin-film materials, including record-high MO figures of merit and improved conventional and un-conventional hysteresis loops of Faraday rotation. The attractive optical, magnetic, and magneto-optic properties obtained in highly bismuth-substituted iron garnet thin-film materials of multiple composition types are relevant in the context of manufacturing next-generation ultra-fast optoelectronic devices, such as light intensity switches and modulators, high-speed flat panel displays, and high-sensitivity sensors.

Keywords: Bi-substituted; RF magnetron; Sputtering; Annealing; Oxygen plasma treatment; Magneto-optic; Faraday rotation; Figure of merit; Hysteresis loop; Imaging; Sensing

1. Introduction

Substitution of bismuth into iron-based garnets enhances the magnetic properties of garnet thin films and monocrystals. The exceptional optical and magneto-optical properties in the near-infrared spectral region, make the bismuth-substituted iron garnets the most promising magneto-optical dielectric ferrimagnetic materials [1-10]. However, the practical application of Bi-substituted iron garnets in the visible and short-wavelength infrared parts of the spectrum is limited, due to high optical absorption (especially in sputtered films) in these spectral regions [11-15]. Also, the most developed practical uses of garnet materials are MO imaging and sensing [14-19]. However, achieving improved garnet material properties to suit an expanding variety of applications, as well as future progress in technological and component-level advancements, are still required. New material system development is likely to be the source of these enhancements. MO thin-film garnet materials (single and multilayer) and nano-structured magnetic photonic crystals (MPCs) have emerged as a cutting-edge research area worldwide [20-30]. Fabrication of high-quality thin films with strong control over their microstructure, surface and interface quality, and optical and magnetic behaviors is required for the successful practical deployment of these garnet materials. The use of RF magnetron sputtering allows for fine

Preprints (www.preprints.org) | NOT PEER-REVIEWED | Posted: 13 September 2022 doi:10.20944/preprints202209.0162.v1

control of thin film deposition process parameters, ensuring the production of high-quality thin films and multilayers [12, 13, 31-37].

In this article, we have monographed our last twelve years of study in the field of Bi-containing ferrite-type garnet materials. We explored the techniques for altering the microstructure of thin films and the ways in which garnet crystals are formed. Some of the material system development results we demonstrated confirm the suitability of several new types and classes of nanocrystalline garnet films for a diverse array of applications including security and digital forensics, biomedical imaging, signal processing, and high-speed optical data processing in communications systems.

2. Materials composition studied, garnet development approaches, technological processes, and characterization techniques

2.1. Studied materials composition and multilayer structures

We have investigated a range of Bi-containing metal-doped iron garnet materials. Table 1 lists the material composition types, the focus of the study, the development approaches used, and the publications resulting from our studies.

Table 1. Types of materials composition, study focus, used methodology, and the best (highest) obtained specific Faraday rotations in the visible region.

Material composition type and multilayer structures	Focus of the study	Methodology	Specific Faraday rotation (°/μm) in the visible wavelength range		Major publication
			532 nm	635 nm	
$(Bi,Dy)_3(Fe,Ga)_5O_{12}$: Bi_2O_3	**The focus was to investigate the effects of additional extra bismuth oxide content that can lead to significant improvements in the optical transparency and specific Faraday rotation of sputtered garnet materials in the visible range.**	**Co-sputtering**	9.8	2.6	Optics express, DOI:10.1364/OE.17.019519 [12]
$Bi_{2.1}Dy_{0.9}Fe_{4.3}Ga_{0.7}O_{12}$	The motivation was to explore a new garnet-film stoichiometry type, which is expected to possess somewhat "intermediate" magnetic anisotropy properties, i.e., having neither the in plane nor perpendicular magnetization direction.	Sputtering	10.12	1.66	Optical materials express, DOI:10.1364/OME.7.000676 [37]
$Bi_3Fe_5O_{12}$:Dy_2O_3	$Bi_3Fe_5O_{12}$: Dy_2O_3 (between 2.7 and 20 vol. % of added dysprosium oxide content) garnet-type nanocomposite thin-films have been prepared to synthesize a garnet material with the possible highest bismuth substitution level approaching 3 formula units and to obtain best MO properties while the thin garnet layers sputtered from a ceramic stoichiometrically-mixed oxide-based $Bi_3Fe_5O_{12}$ target unexpectedly showed negligible MO properties.	Co-sputtering	13.30	3.23	Optical materials express, DOI:10.1364/OME.4.001866 [31]

Preprints (www.preprints.org) | NOT PEER-REVIEWED | Posted: 13 September 2022 doi:10.20944/preprints202209.0162.v1

$Bi_{1.8}Lu_{1.2}Fe_{3.6}Al_{1.4}O_{12}$: Bi_2O_3	This study focused on the fabrication of RF sputtered $Bi_{1.8}Lu_{1.2}Fe_{3.6}Al_{1.4}O_{12}$ and the results of adjusting the optical and magnetic properties of these films utilizing co-sputtering deposition using an additional bismuth oxide target.	Co-sputtering	6.25	1.99	Optical materials express, DOI:10.1364/OME.1.000413 [35]
$Bi_2Dy_1Fe_4Ga_1O_{12}$: $Bi_3Fe_5O_{12}$	The co-deposited all-garnet garnet-mix-type films were synthesized to obtain the ultimate bismuth substitution level without using a single-target $Bi_3Fe_5O_{12}$ sputtering process (which was found to result in films not crystallizing into the garnet phase unless composition-diluted through co-sputtering).	Co-sputtering	8.25	1.52	Procedia Engineering, 76 (2014), 61-73. DOI: 10.1016/j.proeng.2013.09.248 [34]
$Bi_{0.9}Lu_{1.85}Y_{0.25}Fe_{4.0}Ga_1O_{12}$	The motivation was to explore a new type of garnet material stoichiometry, ($Bi_{0.9}Lu_{1.85}Y_{0.25}Fe_{4.0}Ga_1O_{12}$), with a combined substitution of Bi and Lu ions at Yttrium (Y) lattice sites, which has so far not been explored extensively using physical vapor deposition techniques. Special attention was devoted to the synthesis of a garnet layer with its lattice parameter as close as possible to that of $Y_3Fe_5O_{12}$ (YIG), and to obtaining low coercivity for applications requiring magnetization-state switching such as MO imaging.	Sputtering	1.25	0.89	Nanomaterials, DOI: 10.3390/nano8050355 [36]
All-garnet multilayer structures	The goal was to explore the engineering of magnetic properties in garnet multilayers, and especially to identify the ways of adjusting the coercive force and magnetic switching and magnetic anisotropy properties by varying the component layer stoichiometries. The effects of exchange coupling on magnetic switching properties of all-garnet multilayer thin film structures have been studied in detail.	Sequential sputtering	NA		Materials 2015, 8, 1976-1992; DOI:10.3390/ma8041976 [32]
Garnet layer / Oxide layer structures	A new technological approach has been applied for the RF-magnetron sputter deposition and annealing crystallization of Bi-substituted iron garnet films.	Sequential sputtering	~2.7 times increment of MO quality obtained in crystallized films.		Materials 2020, 13, 5113; DOI:10.3390/ma13225113 [33]

We have applied different techniques to deposit garnet layers by using the RF magnetron sputtering technique including co-sputtering (using garnet and oxide targets and pairs of dissimilar garnet-stoichiometry targets), the sequential sputtering technique for

Preprints (www.preprints.org) | NOT PEER-REVIEWED | Posted: 13 September 2022 doi:10.20944/preprints202209.0162.v1

multilayer garnet structures, garnet layers deposited under protective oxide layer, and post-deposition oxygen plasma treatment. After the deposition process, all as-deposited thin-film layers were subjected to a conventional oven annealing processes (which were developed and optimized separately for each of the garnet material types synthesized). The composition-dependent annealing crystallization regimes (crystallization time, process temperatures and temperature-ramping rates) were found by multiple trials and sometimes by designing multi-step reannealing processes. The modified techniques used to prepare the garnet layers in our study are described in the following subsections.

2.2. RF-magnetron sputtering and co-sputtering processes

Bismuth-substituted iron garnet and composite-type films were prepared on glass (Corning 1737) and monocrystalline gadolinium gallium garnet (GGG) substrates using an RF magnetron sputtering and co-sputtering technique in low-pressure (1-2mTorr) at pure argon plasma atmosphere with no extra oxygen input. The deposition rates were monitored during sputtering processes by using a well-calibrated quartz crystal microbalance sensor to monitor the film thickness. For the composite films, the estimated amounts of the volumetric fraction of additional components (garnet or oxides) were calculated from the partial deposition rates from both sputtering targets (base garnet target and other targets). The basic formula that was used to calculate the vol.% fraction of excess additional components (oxides or garnet) for the composite-type layers is described in Refs. [12, 13]. We studied several types of garnet-oxides and all-garnets composite films and reported their best-achieved MO properties [12, 31, 35, 37].

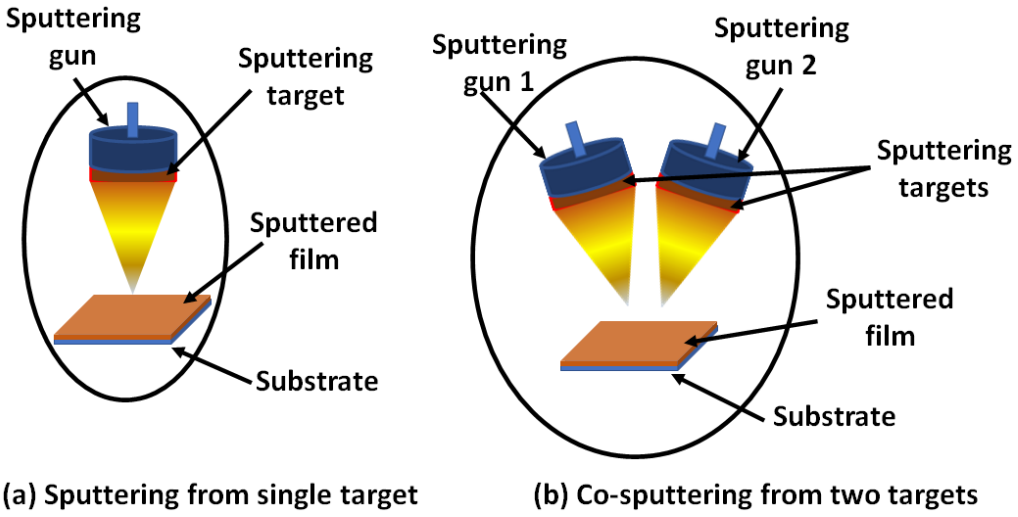

Figure 1. Schematic diagram of RF magnetron sputtering, and co-sputtering techniques used for garnet and composite layers fabrication.

2.3. Sequential sputtering of multilayer garnet structures

Figure 2 shows the schematic diagram of the sequential sputtering process that is used to deposit all-garnet multilayer structures including the material composition types and their magnetic behaviors. In all-garnet multilayer structures, the different layer materials combinations were prepared using the optimized deposition processes and an RF magnetron sputtering system. Inside the multilayer structures, a layer of magneto-soft, low-coercivity material was sandwiched in between two magneto-hard layers possessing strong uniaxial magnetic anisotropy and having a constant thickness. All-garnet multilayer structures employing different garnet-type materials and different layer thicknesses were deposited using RF magnetron sputtering where a sequential sputtering approach was followed (i.e., a single deposition run of each layer using oxide mix-based ceramic sputtering targets and at low-pressure pure-argon plasma). The process parameters, conditions, and optimization of annealing regimes to prepare all-garnet multilayers

Preprints (www.preprints.org) | NOT PEER-REVIEWED | Posted: 13 September 2022 doi:10.20944/preprints202209.0162.v1

structures obtaining very smooth layer interfaces, microstructure morphologies, and microcrack-free surfaces are detailed in Ref. [32].

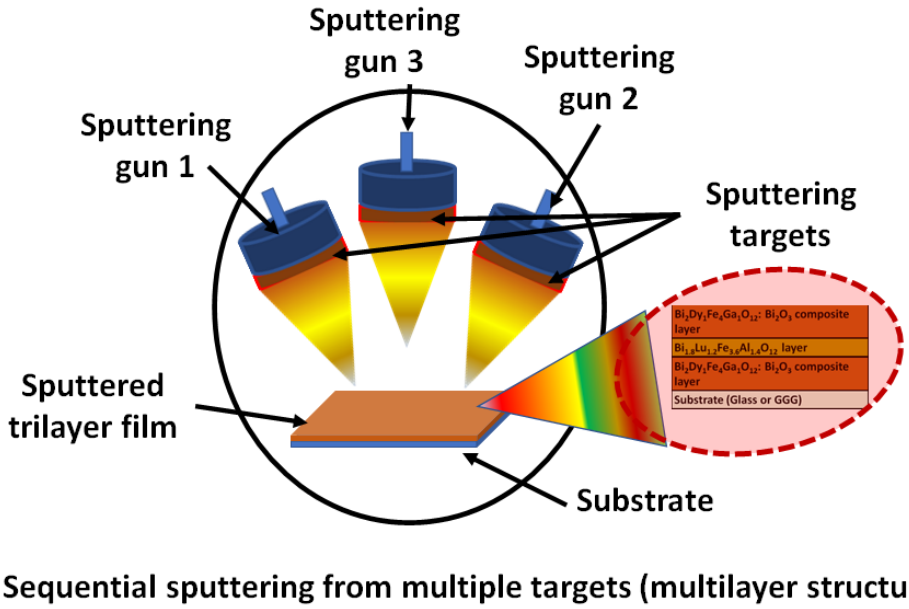

Figure 2. Schematic diagram of the sequential sputtering technique used to deposit the all-garnet multilayer structures.

2.4. Garnet layer formed under a protective oxide layer

Completely new and modified process sequences for annealing crystallization of garnet thin films were studied to improve the properties of highly Bi-substituted iron garnet thin film materials. The manufacture of high-performance ultrathin garnet films requires the provision of a thin (2–20 nm) protective bismuth oxide (Bi_2O_3) layer, which assists in the crystallization of the garnet layer while minimizing the loss of bismuth substitution content. Initially, a 20–60 nm amorphous-phase film of a nanocomposite co-sputtered material type ($Bi_2Dy_1Fe_4Ga_1O_{12}$ + 10-40 vol. % of Bi_2O_3), was deposited onto a GGG or a glass substrate. In the second process stage, a protective bismuth-oxide layer of thickness between 2 nm–20 nm was deposited by using RF magnetron sputtering onto the amorphous nanocomposite films (as schematically presented in Figure 3) before running the annealing crystallization in an air atmosphere, at a (composition-dependent) temperature between 490 °C and 650 °C [33]. Results of the demonstrated garnet layer development are summarized in the next section.

Preprints (www.preprints.org) | NOT PEER-REVIEWED | Posted: 13 September 2022 doi:10.20944/preprints202209.0162.v1

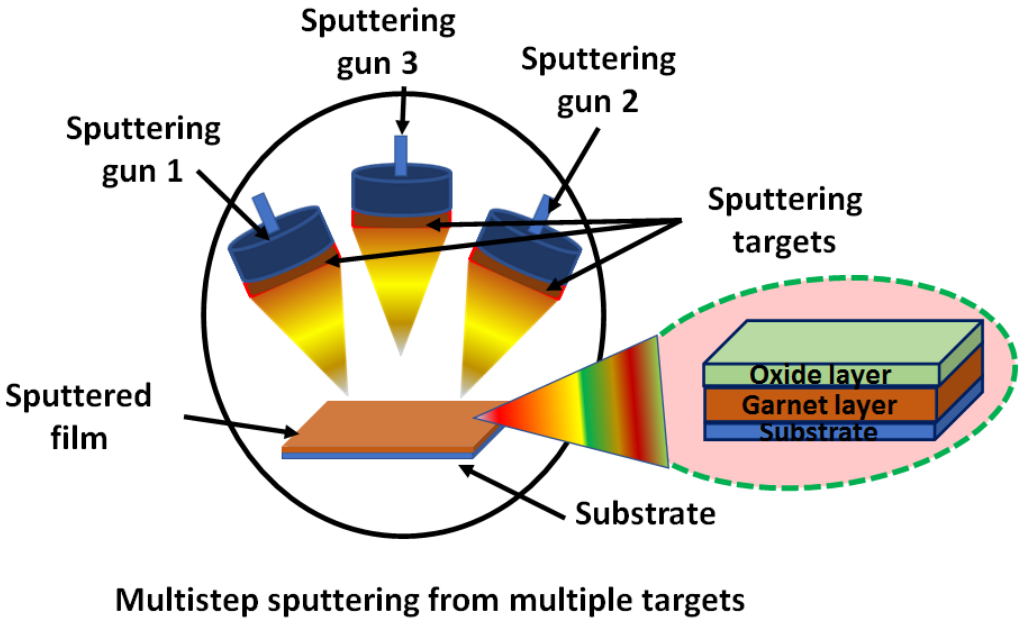

Figure 3. Schematic diagram of a multistep sputtering technique used for garnet/oxide multilayer (garnet layer under protective layer) structures deposition.

2.5. Post-deposition oxygen plasma treatment to as-deposited garnet layer

The oxygen plasma treatment on the as-deposited garnet samples was applied immediately after the deposition. We investigated the effects of post-deposition oxygen plasma treatment on the MO properties of RF sputtered garnet thin-film layers, synthesized using two different types of Bi-substituted garnets. Figure 4 shows the schematic diagram of the flow chart used for post-deposition oxygen plasma treatment of amorphous garnet layers.

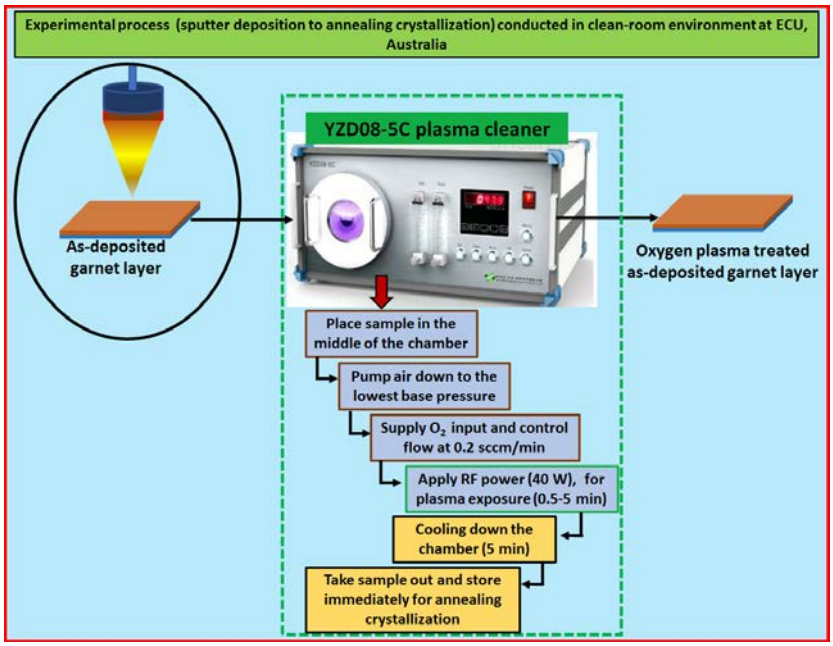

Figure 4. Schematic diagram of the flow chart of oxygen plasma treatment process applied to as-deposited garnet layers.

The oxygen plasma treatment was conducted using YZD08-5C plasma cleaner (purchased through Alibaba.com) for 0.5–5 min. Oxygen plasma-treated (after annealing crystallization) showed better film quality and properties (specific Faraday rotation and MO

 doi:10.20944/preprints202209.0162.v1

figure of merit at 532 nm) than these of the non-treated samples [33]. In addition to all these modified techniques used to deposit garnet and multilayer structures for the improvement and property enhancement of garnet layers in terms of their optical and magneto-optical properties, we also studied and investigated the influence of varying deposition process parameters and the corresponding effects on the garnet layer growth and their properties measured after annealing crystallization as described in subsection 2.6.

2.6. Investigation of deposition process parameter effects on garnet layers

We studied the effects of process parameters associated with the RF magnetron sputter deposition technique on the magneto-optical (MO) properties of highly bismuth-substituted ferrite garnet films of composition type $Bi_{2.1}Dy_{0.9}Fe_{3.9}Ga_{1.1}O_{12}$. The variations in RF sputtering process parameters (substrate stage temperature and rotation rate) influence the properties (films' stoichiometry and MO quality through variations in both the specific Faraday rotation and the optical absorption coefficients) of garnet films. From this study we concluded that the MO characteristics can be tuned and optimized for use in various magnetic field-driven nano-photonics and integrated optics devices with an addition of a flexible and cost-effective approach for the design and development of new, high-quality, and application-specific MO materials for various photonics and integrated-optics applications [38].

2.7. Annealing crystallization processes and material characterization techniques

All the as-deposited garnet layers or multilayer structures were subjected to oven annealing at high temperatures, as the after-deposited garnet layers remain in amorphous phase and show no magnetic or MO properties even if sputtered at high substrate temperatures (up to about 700C, in our group's experience). A conventional temperature/ramp-controlled box furnace oven was used to anneal the as-deposited (amorphous) garnet layers in the air atmosphere. The post-deposition annealing treatment does the softening of the materials, enables the inter-diffusion of metal-oxide precursors, and simultaneously leads (on achieving the necessarily high crystallization process temperature) to the desired changes in the microstructure and other properties of the sputtered garnet layers. The annealing heat treatment of thin films is a sequence of three distinct process steps, including a temperature ramp-up process, holding the specified suitable temperature for a distinct time for isothermal crystallization, and cooling down-ramp at the same or at a different rate compared to the ramp-up rate as can be seen in Figure 5(a). The annealing regimes (temperature and time) optimization are found to be strongly composition dependent. The annealing process durations of 1 to 10 hours have been used, depending on garnet composition type with temperature-ramp process rates of 3-5 ºC/min to crystallize the amorphous (as-deposited) layers into a high-quality nanocrystalline garnet phase with relatively small grain size (tens of nm). The annealing process with the low temperature-ramp rates was preferred to crystallize the amorphous garnet layers as the garnet layers annealed with the high-temperature ramp rate or even rapid thermal annealing process were observed to lead towards micro-cracks and surface damage [39]. However, we have noticed that for some compositions lower cooling down-ramp is the better option to get crystallization of the garnet layer. In addition, we studied the annealing behavior and the crystallization kinetics of garnet-Bi_2O_3 composite films that yielded the estimates of the activation energy of isothermal crystallization for this type of material resulting in a guide for obtaining high-performance garnet films and for the design of optimized thermal processing regimes suitable for the synthesis of highly Bi-substituted garnets using physical vapor deposition methods [40]. The annealing process optimization experiments conducted to find the most suitable annealing regimes (in terms of both the maximum process temperature and crystallization process duration) for the garnet layers and multilayer structures are schematically described in Figure 5(a) can be used as a guide to determine the optimized annealing regimes for almost any garnet or non-garnet film layers as well.

Preprints (www.preprints.org) | NOT PEER-REVIEWED | Posted: 13 September 2022 doi:10.20944/preprints202209.0162.v1

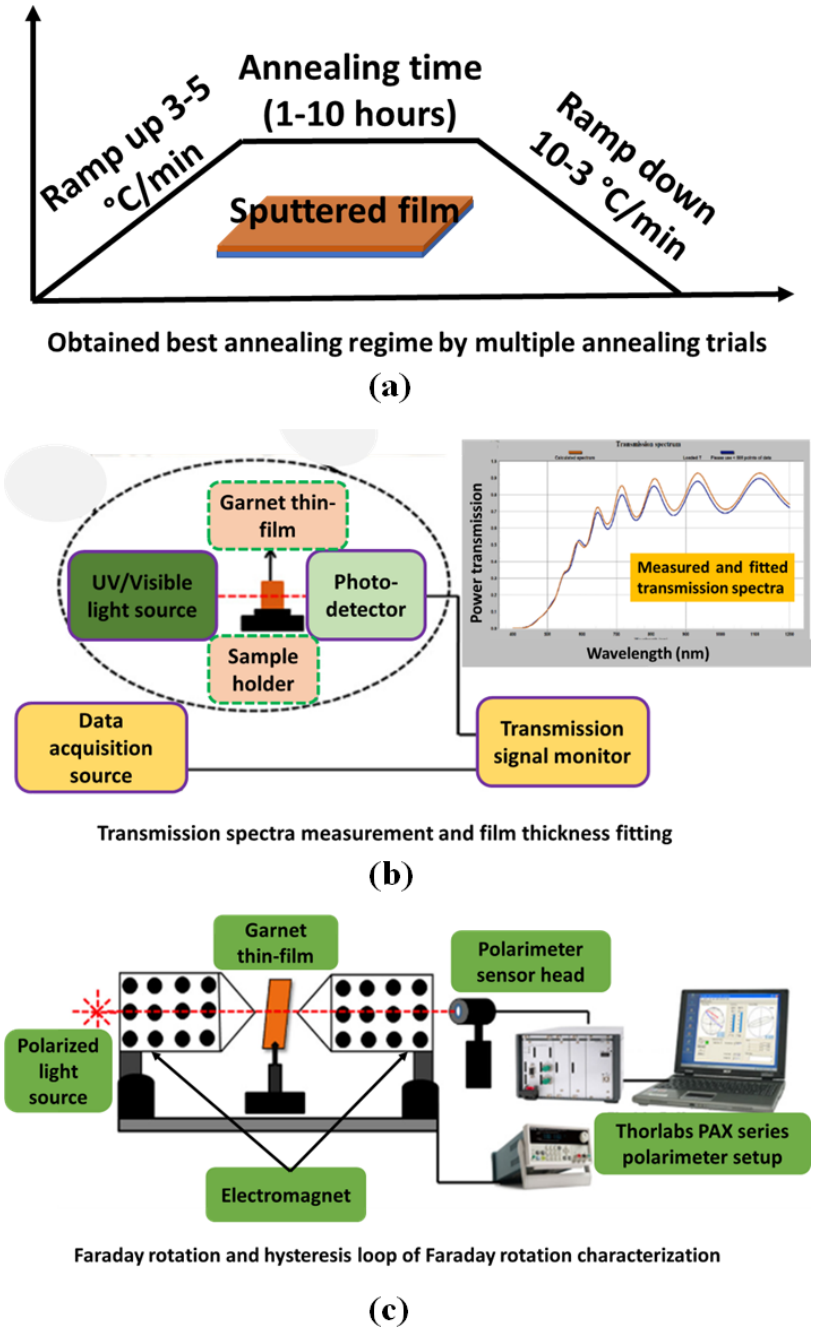

Figure 5. Schematic diagram of the annealing crystallization process of garnet layer (a), measurement of optical transmission spectra to derive the film thickness and absorption coefficient (b), and specific Faraday rotation and hysteresis loop of Faraday rotation characterization methodologies (c) [13].

Optimally annealed and high-quality garnet and composite type garnet thin films were subjected to multi-parameter characterization to investigate the micro-structure, optical, magnetic, and MO properties. The crystal structure and impurity phases were analyzed using X-ray diffractometry (XRD), and energy-dispersive X-ray spectroscopy (EDS) data. Initially, the optical properties of garnet films were investigated by measuring the transmission spectra using a UV/Visible spectrophotometer and by deriving the absorption coefficient spectra. Later we derived accurately the optical constants data for multiple rare-earth doped iron garnets simultaneously with the garnet film thicknesses from the optical transmission spectra employing a combinatorial approach of employing custom-built spectrum-fitting software in conjunction with Swanepoel's envelope method to

Preprints (www.preprints.org) | NOT PEER-REVIEWED | Posted: 13 September 2022 doi:10.20944/preprints202209.0162.v1

overcome the spectral limitations with our previous measurement technique [41]. The magnetic and MO properties of the garnet films were characterized by measuring the Faraday rotation angle (almost across the entire visible spectral region) and Faraday rotation hysteresis loops. The experimental set-up for measuring the optical transmission and specific Faraday rotation is schematically detailed in Figure 5 (b, and c). Other than these characterizations, we performed the magnetic circular dichroism (MCD) measurements for some garnet material composition types with the help of our international research collaborators in the Russian Federation (Prof. V.A. Kotov's Group at the Institute of Radio Engineering and Electronics, Moscow).

3. Results and discussion

A range of MO garnet and composite layer material types (garnet-oxide, garnet-garnet, and multilayer structures) materials with high bismuth content were synthesized, characterized, studied, and evaluated in terms of the optical, and magneto-optical properties. In this section, we would like to present a glimpse of the best achieved optical and MO properties that we have observed and reported in multiple scientific publications. Figure 6 presents an example of obtained optical and MO properties of garnet layers prepared by various development approaches e.g. synthesizing the garnet-oxides composites, applying post-deposition oxygen plasma treatment, and garnet layers deposited using different substrate stage rotation rates (rpm).

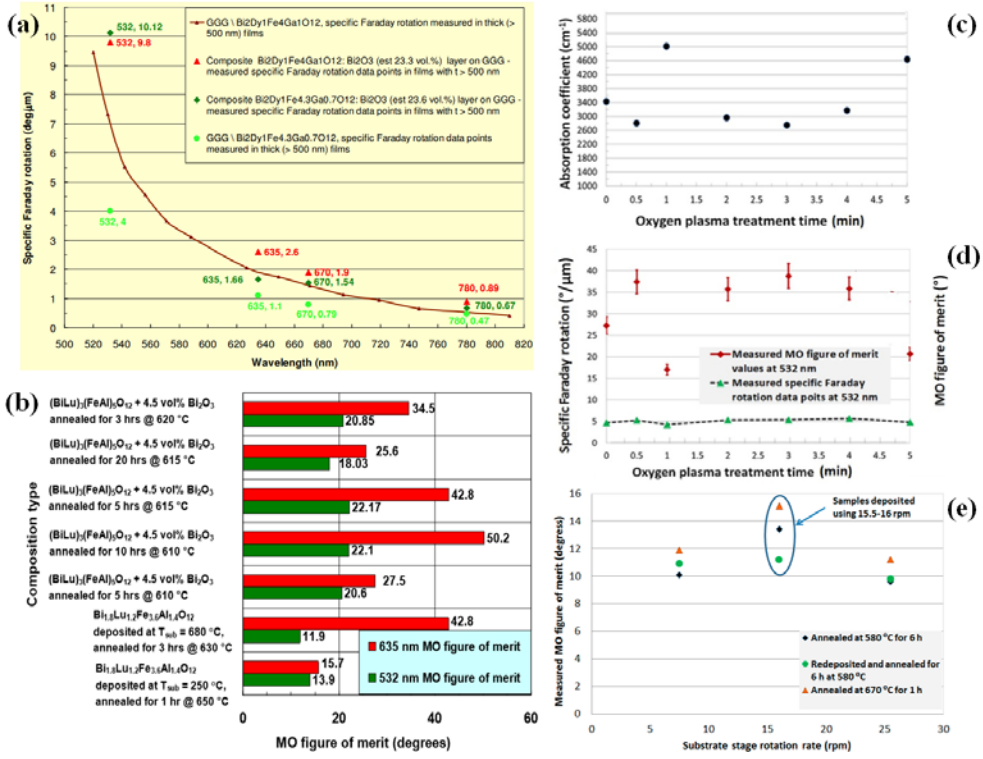

Figure 6. Optimized (best achieved by our group so far) optical and MO properties observed on garnet layers prepared by different development approaches. The best obtained specific Faraday rotation of garnet films ($Bi_2Dy_1Fe_4Ga_1O_{12}$), presented with the measured specific Faraday rotation data points achieved in $Bi_2Dy_1Fe_{4.3}Ga_{0.7}O_{12}$ garnet films and the best performing garnet-Bi_2O_3 composite films (a), measured MO quality factor in terms of the figure of merit of typical $Bi_{1.8}Lu_{1.2}Fe_{3.6}Al_{1.4}O_{12}$ garnet layer and deposited at 250 °C and 680 °C substrate temperature and several best annealed composite $Bi_{1.8}Lu_{1.2}Fe_{3.6}Al_{1.4}O_{12}$: (4.5 vol. % Bi_2O_3) films (b), improved optical and MO properties observed in oxygen plasma treated garnet films, and the garnet layers deposited using various substrate stage rotation rates (rpm) [13, 37, 33, 38].

The obtained material characterization results indicate that the MO properties across the visible spectral range can be significantly improved in composites possessing an

Preprints (www.preprints.org) | NOT PEER-REVIEWED | Posted: 13 September 2022 doi:10.20944/preprints202209.0162.v1

excess of co-sputtered components (metal oxides, or metal doped garnets). High optical absorption in polycrystalline sputtered garnet-composite layers was found compared with epitaxially-grown (LPE) garnet monocrystals. The addition of extra components (bismuth oxide, dysprosium oxide, and others) can lead to significant improvements in the optical transparency to reduce the optical absorption and increase the specific Faraday rotation of sputtered garnet materials in the visible range. The optimally annealed high-quality garnet-composite thin films were found to demonstrate either high specific Faraday rotation (confirming high Bi substitution levels achieved) and/or low optical absorption across large parts of the visible spectral range. Higher transparency across the near-infrared range and significantly lower absorption coefficients across the visible spectral region compared to the garnet layers sputtered using conventional methodologies confirms the hypothesis of developing high-quality nanocomposite oxide-mixed garnet layers for various existing and forward-looking MO applications including sensing and imaging [12, 13, 31, 34].

Figure 7 shows the measured hysteresis loops of various types of garnet-oxide composite films having different volumetric fractions of extra oxide content and multilayer structures.

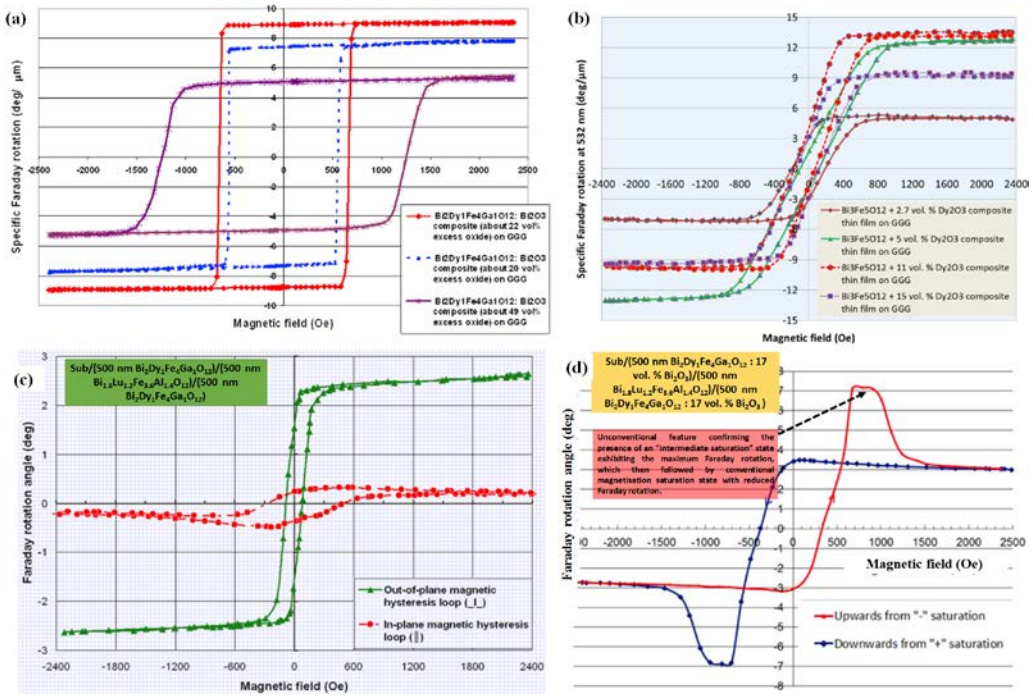

Figure 7. Measured hysteresis loop of Faraday rotation in different types of garnet-oxides composite layers and multilayer structures. The effects of excess oxide content added to the base garnet layers were observed. Measured hysteresis loops of $((Bi,Dy)_3(Fe,Ga)_5O_{12}$: $Bi_2O_3)$ composite films having different volumetric fractions of extra Bi_2O_3 (a), $Bi_3Fe_5O_{12}$: Dy_2O_3) (2.7-15 Vol. %) composite thin films prepared on GGG substrates (b), obtained hysteresis loops from an optimally annealed all-garnet multilayer structure prepared on a GGG (111) substrate with an external magnetic field applied both in perpendicular direction (out-of-plane, green colour curve) and parallel (in-plane, red colour curve) with respect to the film plane of the multilayer structure (c), and an unconventional magnetic hysteresis loop measured in a modified all-garnet multilayer structure. [12, 31, 32, 34].

Various shapes of hysteresis loops of Faraday rotation were observed in our studied all garnet-oxide composites and multilayer structures. The variation and difference of the coercive force and switching field values observed in co-sputtered garnet layers and in different types of all-garnet multilayer structures revealed the possibility of engineering the magnetic characteristics of garnet materials suitable for different ultrafast switching applications or other time-demanding nanotechnological applications. Hysteresis loops of garnet-oxide $((Bi,Dy)_3(Fe,Ga)_5O_{12}$: $Bi_2O_3)$ composite films having different volumetric

Preprints (www.preprints.org) | NOT PEER-REVIEWED | Posted: 13 September 2022 doi:10.20944/preprints202209.0162.v1

fractions of extra Bi_2O_3 were found to be practically square-shaped with the tunable coercive force as presented in Figure 6(a), while the additional dysprosium oxide (Dy_2O_3) to the base garnet material of composition type ($Bi_3Fe_5O_{12}$) led to obtaining hysteresis loops of specific Faraday rotation with tunable and comparatively lower coercive force and saturation magnetization values very attractive for low-switching-field applications (Figure 6b). On the other hand, all-garnet multilayer structures using two record-performance highly-Bi-substituted iron garnet materials having dissimilar magnetic behaviours (magnetic anisotropy types, switching fields and saturation magnetizations) lead to obtaining the potential of custom-engineered magnetic properties that are (to the best of our knowledge) not attainable using single-layer garnet thin films (Figure 6 c, d). The notable and unexpected features of hysteresis loop behaviour confirmed the presence of an "intermediate saturation" state exhibiting the maximum Faraday rotation, which then was followed by conventional magnetisation saturation state with reduced Faraday rotation, at increasing external magnetic fields above about 1 kOe. The final saturated Faraday rotation was observed at near 1.6 kOe, at below 50% of the maximum Faraday rotation angle seen at smaller fields [32]. These exchange-coupled all-garnet multilayer structures are of interest for various emerging applications and future forward-looking research as well. Further studies to achieve better control over the magnetic properties in garnet multilayer structures having different combinations of high-performance garnet materials of various optimized thicknesses as well as stoichiometry types can lead to obtaining more new and unexpected discoveries.

Figure 8 (a-e) depicts the measured spectral dependences of the magnetic circular dichroism (MCD) of ferrite garnet films, in the spectral range from 250 to 600 nm, and the microstructural properties of garnet layers and the results of post-deposition effects on microstructures of the annealed garnet layers.

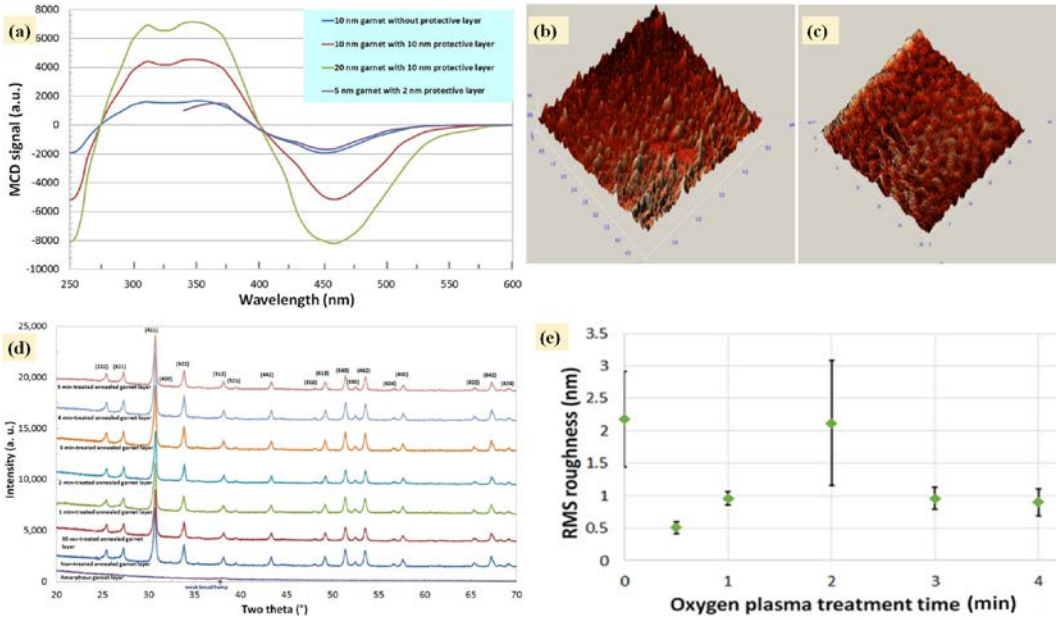

Figure 8. Observed MCD signals from garnet layers prepared under protective layers (a), microstructural properties of garnet-oxide composite (b, c), XRD data, and RMS roughness properties of post-deposition oxygen plasma treated garnet layers followed by optimized annealing crystallization (d, e) [13, 38].

The effects of thin protective Bi_2O_3 layers on the MO properties of ultrathin highly bismuth-substituted dysprosium iron garnet layers have been investigated by performing wavelength-dependent MCD measurements between 250–850 nm at room temperature and at cryogenic temperatures. The magnitude of the MCD signal measured at 450 nm from an oxide-protected annealed film of the garnet-cover layer system was found to be approximately 2.7 times higher than that of an unprotected garnet layer. The MO quality

 doi:10.20944/preprints202209.0162.v1

properties of garnet thin films were also found comparatively better on those garnet layers that were subjected to the oxygen plasma treatment just after the deposition process. Assuming that the pre-diffusion of the oxygen from plasma into garnet film volume occurring before the annealing crystallization process, the plasma treatment could lead to better (faster) compensation of oxygen loss occurring during sputtering, thus preventing the excessive formation of non-garnet material phases during annealing (as can be confirmed from the RMS roughness characterization). These effects and processes still require more investigation using slightly different or any other available garnet film compositions.

4. Conclusions

We have extensively investigated and described multiple different approaches to the synthesis of high-quality, highly bismuth-substituted magneto-optic ferrite garnet layers of different composition types not extensively described in the current literature. The various material system development results achieved led to demonstrating the application-specific and highly customizable magnetic and MO characteristics in garnet films and thin magnetic multilayers, which is of interest in various practical application areas, from magnetoplasmonics to the development of multiple sensors, polarization control, and light intensity modulator systems reliant on ultrafast magnetic switching and magnetic field sensitivity.

Author Contributions: Conceptualization, M.N-E-A.; methodology, M.N-E-A.; M.V.; and K.A.; software, M.N-E-A.; M.V.; and K.A.; validation, M.N-E-A.; M.V.; and K.A.; formal analysis, M.N-E-A.; M.V.; and K.A.; investigation, M.N-E-A.; and M.V.; resources, M.N-E-A.; M.V.; and K.A.; data curation, M.N-E-A.; M.V.; and K.A.; writing—original draft preparation, M.N-E-A.; writing—review and editing, M.N-E-A.; and M.V.; visualization, M.N-E-A.; M.V.; and K.A.; supervision, M.V.; and K.A.; project administration, K.A.; funding acquisition, M.N-E-A.; M.V.; and K.A. All authors have read and agreed to the published version of the manuscript.

Funding: This research received no external funding.

Institutional Review Board Statement: Not applicable.

Informed Consent Statement: Not applicable.

Data Availability Statement: Not applicable.

Acknowledgments: We would like to acknowledge the academic support of School of Science, Edith Cowan University, Australia. We would also like to acknowledge our international research collaborators from the Russian Federation, Germany, Switzerland, and India.

Conflicts of Interest: The authors declare no conflict of interest.

Appendix A

The appendix contains a list of publications made by our group that related to the study of synthesis and development of various garnet materials towards their practical applications but are not cited in this article. This list will be useful for the readers, the scientific community, and the government and commercial industries.

1. **YIG: Bi_2O_3 nanocomposite thin films for magneto-optic and microwave applications**. *Journal of nanomaterials*, 2015, Article ID 182691, doi.org/10.1155/2015/182691.
2. Synthesis, characteristics and material properties dataset of Bi:DyIG-oxide garnet type nanocomposites. *Journal of nanomaterials*, 2015, Article ID 127498, doi.org/10.1155/2015/127498.
3. Growth, characterization, and properties of $Bi_{1.8}Lu_{1.2}Fe_{3.6}Al_{1.4}O_{12}$ garnet films prepared using two different substrate temperatures. *Int. J. Materials Engineering Innovation*, Vol. 5, No. 3, 2014, https://doi.org/10.1504/IJMATEI.2014.064275.
4. Physical properties and behaviour of highly Bi-substituted magneto-optic garnets for applications in integrated optics and photonics. *Advances in Optical Technologies*, volume 2011, Article ID 971267, 7 pages, doi:10.1155/2011/971267.

5. Nano-structured magnetic photonic crystals for magneto-optic polarization controllers at the communication-band wavelengths. *Opt. Quant. Electron*. 41, 661-669, 2009.
6. Analysis, optimization, and characterization of magnetic photonic crystal structures and thin-film material layers. *Technologies*, 2019, 7 (3), 49, doi.org/10.3390/technologies7030049.
7. Sensing of surface and bulk refractive index using magnetophotonic crystal with hybrid magneto-optical response. *Sensors*, 2021, 21, 1984.
8. Magneto-optic properties of ultrathin nanocrystalline ferrite garnet films in the 8K to 300K temperature interval. *Journal of nanomaterials*, 2018, Article ID 7605620, doi.org/10.1155/2018/7605620.
9. **Properties of magnetic photonic crystals in the visible spectral region and their performance limitations**. *Photonics and Nanostructures - Fundamentals and Applications*, 2018, Vol. 28, pp 12-19, doi.org/10.1016/j.photonics.2017.11.003.
10. High-Q surface modes in photonic crystal/iron garnet film heterostructures for sensor applications. *JETP Letters*, 2016, Vol. 104, No. 10, pp. 679–684, doi.org/10.1134/S0021364016220094.
11. **Transverse magnetic field impact on waveguide modes of photonic crystals**. *Optics Latter*, 2016, Vol. 41 (16), pp 3813-3816, DOI: 10.1364/OL.41.003813.
12. Tunable optical nanocavity of iron-garnet with a buried metal layer. *Materials*, 2015, 8(6), 3012-3023; doi:10.3390/ma8063012.
13. Magneto-optic properties of ultrathin bismuth-substituted ferrite garnet films obtained by RF magnetron sputtering method. *J. Comm. Tech. Electron*., 2014, 10.1134/S1064226914110096.
14. **Magneto-Photonic intensity effects in hybrid metal-dielectric structures**. *Physical Review B*, 89, 045118 (2014), doi.org/10.1103/PhysRevB.89.045118.
15. **Plasmon mediated magneto-optical transparency**. *Nature Communications*, 4:2128, doi: 10.1038/ncomms3128 (2013).
16. Tuning of the transverse magneto-optical Kerr effect in magneto-plasmonic crystals. *New J. Phys*., 15, 075024, (2013), doi:10.1088/1367-2630/15/7/075024.
17. **Magnetic heterostructures with low coercivity for high-performance magneto-optic devices**. *J. Phys. D: Appl. Phys*., 46 035001, (2013), doi:10.1088/0022-3727/46/3/035001. Impact Factor- 2.829, Cite Score- 2.75.

References

1. Zvezdin, A. K.; Kotov, V. A. Modern Magnetooptics and Magnetooptical Materials (Institute of Physics Publishing, Bristol and Philadelphia, ISBN075030362X, 1997.
2. Hansteen, F. Ultrafast optical control of magnetization in ferrimagnetic garnets, PhD thesis, 2006, http://www.hansteen.net/thesis.pdf
3. Bi, L.; Hu, J.; Jiang, P.; Kim, H.S.; Kim, D.H.; Onbasli, M.C.; Dionne, G.F.; Ross, C.A. Magneto-optical thin films for on-chip monolithic integration of non-reciprocal photonic devices, Materials, 2013, 6, 5094-5117.
4. Scott, G.B.; Lacklison, D.E.; Magnetooptic properties and applications of Bismuth substituted iron garnets, IEER Trans. Magn. 1976, 12, 292-311.
5. Nistor. I. Development of magnetic field sensors using Bisbuth-substituted garnets thin films with in-plane magnetization, Phd, thesis, 2006, University of Maryland.
6. Kang, S. Advanced magneto-optical materials and devices, PhD thesis, 2007, The Pennsylvania University.
7. Gomi, M.; Tanida, T.; and Abe, M. RF sputtering of highly Bi-susbtituted garnet films on glass substrates for magneto-optic memory, I. Appl. Phys. 1997, 81(8), 5653-5655.
8. Buhrer, C.F. Faraday rotation and dichroism of bismuth calcium vanadium iron garnet, J. Appl. Phys., 1969, Vol. 40(11), 4500-4502.
9. Danish, A. W. Study on preparation and characterization of Bismuth substituted Gadolinium iron garnet thin films by metal orgaini decomposition method, Phd thesis, 2017, Tokyo University of Agriculture and Technology.
10. Deb, M.; Popova, E.; Keller, N. Different magneto-optical response of magnetic sublattices as a function of temperature in ferrimagnetic bismuth iron garnet films, Phys. Rev. B, 2019, 100, 224410.

11. Kahl. S. Bismuth iron garnet films for magneto-optical photonic crystals, PhD thesis, 2004, https://www.diva-portal.org/smash/get/diva2:9551/FULLTEXT01.pdf.
12. M. Vasiliev, M. Nur-E-Alam, V. A. Kotov, K. Alameh, V. I. Belotelov, V. I. Burkov, and A. K. Zvezdin RF magnetron sputtered $(BiDy)_3(FeGa)_5O_{12}$:Bi_2O_3 composite garnet-oxide materials possessing record magneto-optic quality in the visible spectral region, October 2009, Optics Express 17(22):19519-35.
13. Alam. M. High Performance Magneto-Optic Garnet Materials for Integrated Optics and Photonics, PhD thesis, 2012, https://ro.ecu.edu.au/theses/528.
14. Kang, S.; Yin, S.; Adyam, V.; Li, Q.; Zhu, Y. $Bi_3Fe_4Ga_1O_{12}$ Garnet Properties and Its Application to Ultrafast Switching in the Visible Spectrum, IEEE Trans. Magn. 2007, 43, 3656–3660, doi:10.1109/TMAG.2007.900874.
15. Liu, X.; Yang, Q.; Zhang, D.; Wu, Y.; and Zhanga, H. Magnetic properties of bismuth substituted yttrium iron garnet film with perpendicular magnetic anisotropy, AIP Advances, 9, 115001 (2019); doi: 10.1063/1.5122998.
16. Zanjani, S.M.; and Onbasli, M.C. Thin film rare earth iron garnets with perpendicular magnetic anisotropy for spintronic applications. AIP Advances, **9**, 035024 (2019); https://doi.org/10.1063/1.5079738.
17. Eschenfelder, A. Magnetic Bubble Technology; Springer: New York, NY, USA, 1980.
18. Aichele, T.; Lorenz, A.; Hergt, R.; Görnert, P. Garnet layers prepared by liquid phase epitaxy for microwave and magneto-optical applications—A review. Cryst. Res. Technol. 2003, 38, 575–587, doi:10.1002/crat.200310071.
19. Gomi, M.; Tanida, T.; Abe, M. RF sputtering of highly Bi-substituted garnet films on glass substrates for magneto-optic memory. J. Appl. Phys. 1985, 57, 3888–3890, doi:10.1063/1.334905.
20. Inoue, M. Magnetophotonic crystals, Mater. Res. Soc. Symp. Proc. Vol. 834 © 2005 Materials Research Society.
21. Hu, S.; Guo, Z.; Dong, L.; Deng, F.; Jiang, H.; and Chen, H. Enhanced magneto-optical effect in heterostructures composed of epsilon-near -zero materials and truncated photonic crystals, Front. Mater., 2022, https://doi.org/10.3389/fmats.2022.843265.
22. Wu, Z. Planar magneto-photonic and gradient-photonic structures: crystals and metamaterials,, PhD thesis, 2010, https://digitalcommons.mtu.edu/cgi/viewcontent.cgi?article=1120&context=etds.
23. Da, H., Li, Z., 'Manipulating nematic liquid crystals-based magnetophotonic crystals, 2009, In G. Tkachenko (ed.), New Developments in Liquid Crystals, IntechOpen, London. 10.5772/9690.
24. Fathi F, Rashidi MR, Pakchin PS, Ahmadi-Kandjani S, Nikniazi A. Photonic crystal based biosensors: Emerging inverse opals for biomarker detection. Talanta. 2021 Jan;221:121615. DOI: 10.1016/j.talanta.2020.121615. PMID: 33076145; PMCID: PMC7466948.
25. Sohlstrom, H. Fibre optic magnetic field sensors utilizing iron garnet materials, PhD thesis, 1993, School of Electrical Engineering, Royal Institute of Technology, Stockholm, Sweden.
26. Jha, A.R. Rare earth materials, properties and applications. CRC press, Taylor & Francis group, Boca Raton, London, New York. https://ftp.idu.ac.id/wp-content/uploads/ebook/tdg/BUKU%20REE/Rare%20Earth%20Materials%20Properties%20and%20Applications%20by%20Jha,%20A.R.%20(z-lib.org).pdf
27. Mitra, A. Structural and magnetic properties of YIG thin films and interfacial origin of magnetisation suppression, PhD thesis, 2017, University of Leeds, https://etheses.whiterose.ac.uk/18696/1/Arpita%20Mitra_FinalThesis.pdf
28. Zhukov, A.; Inoue, M.; Phan, M.H.; and Shavrov, V. Advanced Magnetic Materials, Volume 2012, Article ID 385396, 2 pages
29. Lou, G.; Kato, T.; Iwata, S.; and Ishibashi, T. Magneto-optical properties and magnetic anisotropy of $Nd_{0.5}Bi_{2.5}Fe_{5-y}Ga_yO_{12}$ thin films on glass substrates," Opt. Mater. Express 7, 2248-2259 (2017)
30. Jesenska, E.; Yoshida, T.; Shinozaki, K.; Ishibashi, T.; Beran, L.; Zahradnik, M.; Antos, R.; Kučera, M.; and Veis, M. Optical and magneto-optical properties of Bi substituted yttrium iron garnets prepared by metal organic decomposition," Opt. Mater. Express 6, 1986-1997 (2016)
31. Nur-E-Alam, M.; Vasiliev, M.; and Alameh, K. $Bi_3Fe_5O_{12}$: Dy_2O_3 composite thin film materials for magneto-photonics and magneto-plasmonics, Optical materials Express, Vol. 4, Issue 9, pp. 1866-1875 (2014), doi.org/10.1364/OME.4.001866.
32. Nur-E-Alam, M.; Vasiliev, M.; Kotov, V.A.; Balabanov, D.E.; Akimov, I.A. and Alameh, K. Properties of exchanged coupled all-garnet magneto-optic thin film multilayer structures, Materials, 2015, 8(4), 1976-1992; doi:10.3390/ma8041976.
33. Kotov, V.A.; Nur-E-Alam, M.; Vasiliev, M.; Alameh, K.; Balabanov, D.E.; and Burkov, V. I. Enhanced magneto-optic properties in sputtered Bi- containing ferrite garnet thin films fabricated using oxygen plasma treatment and metal oxide protective layers, Materials, 2020, 13(22):5113.
34. Nur-E-Alam, M.; Vasiliev, M.; Kotov, V.A.; and Alameh, K. Recent developments in magneto-optic garnet-type thin-film materials synthesis, Procedia Engineering 76 (2014) 61–73, DOI: 10.1016/j.proeng.2013.09.248, 2014.
35. Nur-E-Alam, M.; Vasiliev, M.; Kotov, V.A.; and Alameh, K. Highly bismuth-substituted, record-performance magneto-optic garnet materials with low coercivity for applications in integrated optics, photonic crystals, imaging and sensing, Optical materials Express, Vol. 1, Issue 3, pp. 413-427 (2011), doi.org/10.1364/OME.1.000413.
36. Nur-E-Alam, M.; Vasiliev, M.; Belotelov, V.; and Alameh, K. Properties of ferrite garnet $(Bi, Lu, Y)_3(Fe, Ga)_5O_{12}$ thin film materials prepared by RF magnetron sputtering, Nanomaterials, 2018, 8, 355; doi:10.3390/nano8050355.
37. Nur-E-Alam, M.; Vasiliev, M.; and Alameh, K. High-performance RF-sputtered Bi-substituted iron garnet thin films with almost in-plane magnetization, Opt. Mat. Express, 2017, Vol. 7 (3), pp. 676-686, https://doi.org/10.1364/OME.7.000676
38. Nur-E-Alam, M.; Vasiliev, M.; and Alameh, K. Influence of substrate stage temperature and rotation rate on the magneto-optical quality of rf-sputtered $Bi_{2.1}Dy_{0.9}Fe_{3.9}Ga_{1.1}O_{12}$ garnet thin films, Appl. Sci. 2018, 8, 456; doi:10.3390/app8030456.

39. Vasiliev, M.; Nur-E-Alam, M.; Alameh, K.; Premchander, P.; Lee, Y.T.; Kotov, V.A.; and Lee, Y. P. Annealing behaviour and crystal structure of RF-sputtered Bi-substituted dysprosium iron-garnet films having excess co-sputtered Bi-oxide content, J. Phys. D: Appl. Phys. 44 (2011) 075002
40. Nur-E-Alam, M.; Vasiliev, M.; Alameh, K.; and Kotov, V.A. Synthesis of high-performance magnetic garnet materials and garnet-bismuth oxide nanocomposites using physical vapor deposition followed by high-temperature crystallization, Pure Appl. Chem. , Vol. 83, No. 11, pp. 1971–1980, 2011. doi:10.1351/PAC-CON-11-02-02
41. Nur-E-Alam, M.; Vasiliev, M.; and Alameh, K. Optical constants of rare-earth substituted amorphous oxide-mix-based layers deposited to enable synthesis of magneto-optic garnets, https://doi.org/10.1016/j.optmat.2019.109309.